Sylvain Ranvier, Jarmo Kivinen, and Pertti Vainikainen. 2007. Millimeter-wave MIMO radio channel sounder. IEEE Transactions on Instrumentation and Measurement, volume 56, number 3, pages 1018-1024.

Millimeter-Wave MIMO Radio Channel Sounder

Sylvain Ranvier, Jarmo Kivinen, and Pertti Vainikainen, *Member, IEEE*

***Abstract*—Nowadays, the need for high-data-rate-communication channels is increasing and will ineluctably continue to increase in the future. From a theoretical point of view, the multiple input multiple output (MIMO) approach seems to be one of the best solutions to provide such a high capacity. This paper presents a millimeter-wave MIMO channel measurement system developed in the Radio Laboratory of Helsinki University of Technology. The system is based on a sounder and virtual antenna arrays: The antenna arrays are obtained by two 2-D scanners which shift a single transmit antenna and a single receive antenna. Measurements in line of sight (LOS) and non-LOS are reported from what the MIMO channel capacity is calculated for various antenna array sizes. Furthermore, from the same measurements, the direction of departure and direction of arrival are estimated.**

***Index Terms*—Antenna array, millimeter-wave measurement, multiple input multiple output (MIMO) measurement, radio channel measurement, radiowave propagation.**

I. Introduction

THE USE of the wideband 60-GHz radio propagation channel will allow high data rates in future communication systems [1]. Indeed, this frequency range offers huge bandwidths and, due to the oxygen absorption, improves frequency reuse compared to lower frequencies. Furthermore, at 60 GHz, the wavelength is small; therefore, small size antenna arrays are feasible. Therefore, an antenna array with at least ten elements could be implemented in a small area, e.g., corner of laptop, personal data assistant, or mobile phone, to be used either for multiple input multiple output (MIMO) diversity (transmit/receive diversity) or spatial multiplexing.

However, the achievable capacity of MIMO systems is defined by the availability of parallel propagation channels in a multipath environment. Consequently, radio channel measurements at 60 GHz are needed to characterize these parallel separate propagation paths at this frequency in order to develop a reliable prediction model for 60-GHz radio channel.

So far, most of the solutions for characterizing the radio channel in the 60-GHz band are based on a vector network analyzer like in [2] and [3], where the measurement range is usually limited to a few meters, and the characterization of the channel is slow, limiting the possibilities to perform multichannel measurement required for MIMO.

Manuscript received June 15, 2005; revised October 16, 2006. This work was supported by the Academy of Finland and the Nokia Foundation.

S. Ranvier and P. Vainikainen are with the Radio Laboratory/SMARAD, Helsinki University of Technology, 02015 Espoo, Finland (e-mail: sylvain.ranvier@tkk.fi; pertti.vainikainen@tkk.fi).

J. Kivinen is with the Elektrobit OY, 9 A 02700 Kauniainen, Finland (e-mail: jarmo.kivinen@elektrobit.com).

Color versions of one or more of the figures in this paper are available online at http://ieeexplore.ieee.org.

Digital Object Identifier 10.1109/TIM.2007.894197

In this paper, we present a MIMO measurement system with a center frequency at 61.3 GHz, which enables the characterization of the radio channel [estimation of the capacity, direction of departure (DoD), and direction of arrival (DoA)].

To our knowledge, so far, our measurement system is the only millimeter-wave MIMO sounder in the world.

The organization of this paper is as follows: Section II presents the different possibilities to design antenna arrays and explains our choice. In Section III, the measurement setup is described. The measurements and the experimental results are presented in Sections IV and V, respectively. Section VI concludes this paper.

II. Antenna Array

At millimeter-wave range, one of the major issues in the implementation of the MIMO measurement system is to design a proper antenna array. There are basically two solutions.

The first one includes building two antenna arrays: one for the transmitter and one for the receiver. In this case, in order not to increase the complexity of the system (parallel architecture and calibration of the parallel branches), we must have switches that select each element of the array independently, as described in [4]. For the switches at this frequency band, two technologies are available: GaAs monolithic microwave integrated circuit (MMIC) switches and microelectromechanical system (MEMS) switches. The main problem of GaAs MMIC switches is the difficulty of integration. In order to enable measurement in the angular domains, the distance between two adjacent antennas must be a half wavelength or less. In this case, in the 61.3-GHz frequency range, antennas have to be integrated on the same substrate as the switches. The other problem is the insertion loss (typically between 1.5- and 2-dB insertion loss for single-pole double-throw (SPDT) switch). Then, for a 64-element array ($8 \cdot 8$), there is about 10-dB loss. Using MEMS switches allows better insertion loss (typically less than 0.5 dB for SPDT switch). On the other hand, custom-designed MEMS switches are quite expensive, and as for the GaAs MMIC switches, the integration with antennas on the same substrate is quite difficult.

The second solution, which consists of creating a "virtual antenna array" using a matrix shifter (e.g., [5]), was chosen. The term "virtual antenna array" is used because there are no real arrays. There are only one antenna for the transmitter and one antenna for the receiver. These antennas are moved in order to get a channel matrix. The advantages of this solution are good link budget (no losses in switches and antennas with relatively high gain), the relatively low cost compared to the use of MEMS switches, and freedom of choice of the antenna array configurations.

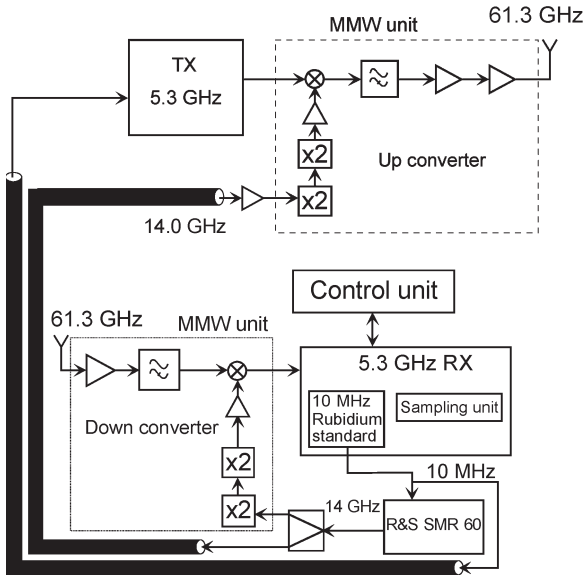

Fig. 1. Signal-based measurement setup description.

The most critical point when creating virtual antenna arrays is the duration of the measurement. The first problem is the phase drift between the transmitter and the receiver. The second one is that the channel must be static during the measurement. As the wavelength is about 5 mm, even someone breathing in the channel under test can dramatically affect the results. Practically, that means that the measurements have to be done in empty rooms (without anybody inside).

Several possibilities were studied to create the virtual antenna arrays. Among them, there are the use of linear stages, rotational stages, and the use of both (helical movement). The advantages of rotational stages are that they can perform the measurement very fast and that they are relatively cheap, compared to linear stages (two linear stages are needed to form a circle). The problems of these rotational stages are that only a circular array can be done and that all the cables connected to the up/down converters have to be rotated, which is, in practice, impossible. For these reasons, linear stages were chosen. The problems of these stages are that they are relatively slow when high accuracy is required and that they are rather expensive. On the other hand, these stages allow all possible array configurations in two dimensions.

III. Measurement Setup

The wideband MIMO system is based on a 5.3-GHz sounder developed at the Helsinki University of Technology [6], [7], which uses direct sequence waveform.

Then, the up converter (which converts 5.3 GHz into 61.3 GHz) and the down converter (which converts the 61.3 GHz into 5.3 GHz) are added (see Fig. 1). The frequency of the local oscillator is 14 GHz. These up and down converters are small enough so that they can be moved with the linear stages to create virtual antenna arrays (see Fig. 2). The phase continuity is a major concern when defining the direction of arrival [8]. In order to synchronize the transmitter and the receiver and avoid phase drifts, the same 14-GHz synthesizer

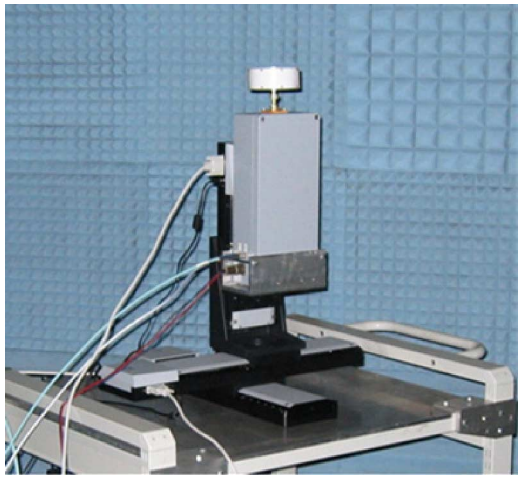

Fig. 2. Picture of the transmitter (up converter and antenna) on the scanner in the anechoic chamber.

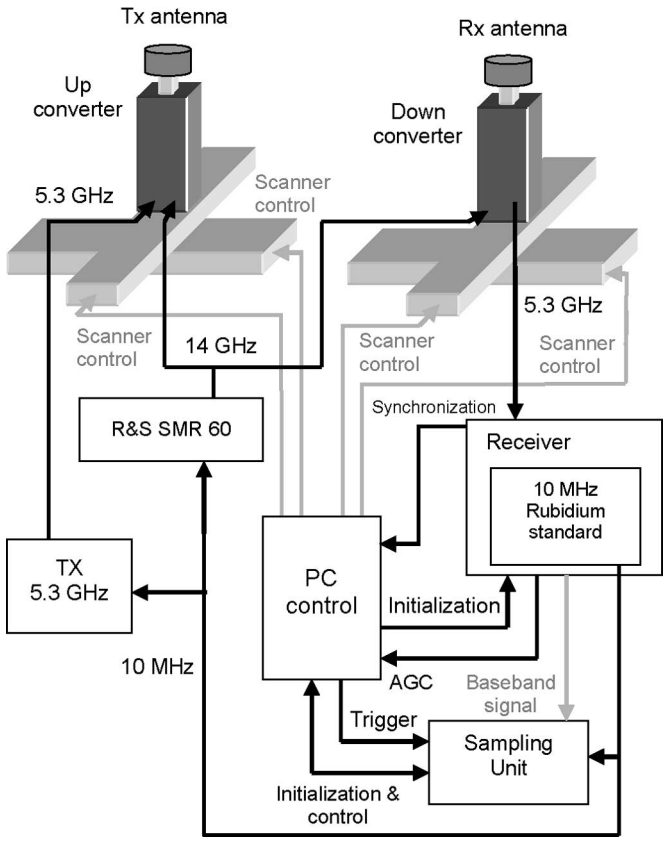

Fig. 3. Control-based measurement setup description.

is used. Then, a 25-m-low loss cable is used to connect the receiver to the synthesizer. The loss in this cable is about 15 dB at 14 GHz. The same 10-MHz Rubidium standard is used as a reference for both the transmitter and the receiver (see Fig. 1). The output power of the up converter is 17 dBm, which enables non-line-of-sight (NLOS) measurements.

The data sampling unit, the receiver, and the matrix shifters are controlled by a computer, as shown in Fig. 3. The triggering of the sampling unit is based on the position of the antennas on the linear stages and a synchronization signal.

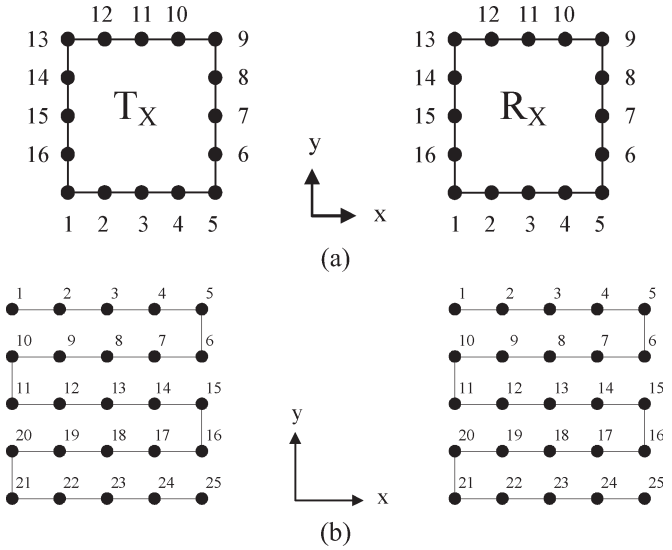

Fig. 4. (a) Antenna arrays configuration (16 elements). (b) Antenna arrays configuration (25 elements).

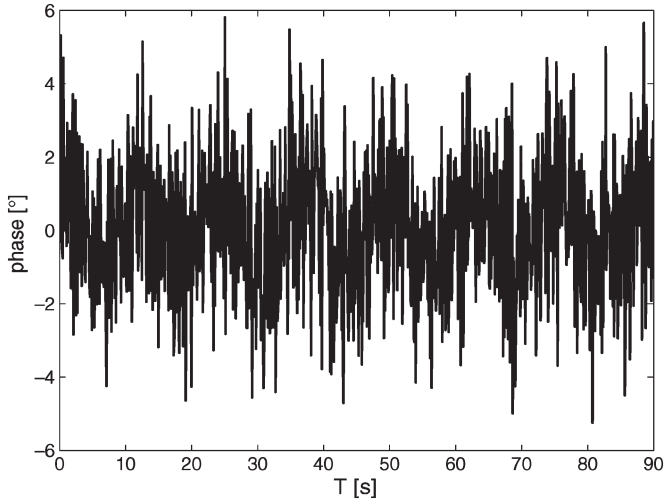

Fig. 5. Phase drift of the setup in back-to-back measurement.

Because of the 25-m-long cable, the measurement range is restricted in a circle with radius of 25 m. Nevertheless, within this area, quite significant data can be obtained at 60 GHz, because the link ranges in future radio systems cannot be very long.

The virtual antenna arrays at the transmitter and receiver are similar. They are either empty squares with five elements along each edge (a total of 16 elements), as depicted in Fig. 4(a), or full squares with 5×5 elements, as depicted in Fig. 4(b). The 16-element array (five elements along each edge) was chosen as a compromise between accuracy in the angular domain and the duration of the measurement. The 25-element array (5×5 elements) was chosen in order to have much larger number of channels, which required to calculate the channel capacities. The space between two elements is λ or $\lambda/4$, depending on the measurements (Section IV). Therefore, a $16 \cdot 16$ channel matrix (16 positions for transmitter and 16 positions for receiver) or $25 \cdot 25$ channel matrix (25 positions for transmitter and 25 positions for receiver) are obtained. The scanners at both the transmitter and receiver are manufactured by Physik Instrumente GmbH. The resolution is 0.1 μm, and the repeatability is 1 μm. Then, the accuracy is $2.04 * 10^{-4}\lambda$ ($= 0.0735^\circ$ of the phase) at 61.3 GHz.

Another way to perform the MIMO channel measurements at millimeter-wave frequency is to use a vector network analyzer (VNA). It allows wider bandwidth than the channel sounder. On the other hand, the channel sounder is much faster. Furthermore, at millimeter-wave frequency, the channel measurement with VNA cannot be done without frequency converters, because long cables cannot be used. In order to perform fast measurements, the channel sounder was chosen instead of the VNA.

IV. Measurements

We first measured the phase stability during 90 s in order to be sure that the measurement was possible (Fig. 5). The rms value of the phase drift between the transmitter and the receiver is 2° within 90 s. Therefore, the phase stability is good enough to calculate later the capacity of the radio channel [9]. When considering the phase during a longer time, it can be seen that the phase is oscillating with a period of about 70 min and a peak-to-peak value of 25°. For this reason, the measurements were restricted to 90 s, which is a compromise between the relative stability of the system and the time needed to measure sufficient number of elements in the antenna arrays. The reason of the very slow oscillations seems to be the temperature regulation of the phase-locked loops of the 5-GHz sounder.

Two identical omnidirectional biconical antennas are used at the transmitter and the receiver. The half power beam width is 11° in the elevation plane, and the gain of each antenna is 5 dBi. For all the measurements, the antennas were positioned at 1.5 m above the floor level.

In the NLOS measurements, the receiver was kept in a room, while the transmitter was moved to 24 different positions in a corridor (Fig. 6). We used the 25-element antenna array [Fig. 4(b)], with a distance between elements equal to λ. This measurement led to the calculation of MIMO capacity (Section V).

In the LOS configuration, using the 16-element antenna arrays [Fig. 4(a)], the measurements with and without obstacle were made in a room containing many electronic devices (Fig. 6). In both cases, the distance between the centers of the antenna arrays was 3.2 m. The distance between elements was $\lambda/4$ in order to reduce the level of the spurious responses of the antenna arrays. The obstacle was a square absorber for a millimeter-wave frequency (Eccosorb VFX-NRL2) of size $50 *$ 50 cm placed at a distance equal to the TX and RX.

V. Results

A. Directional Estimation

In Fig. 7, the TX and RX beam forming responses of the $16 \cdot 16$ channel matrix in the LOS case (see Fig. 6) are presented. The antenna array configuration is shown in Fig. 4(a). They are calculated using the beam forming independently in

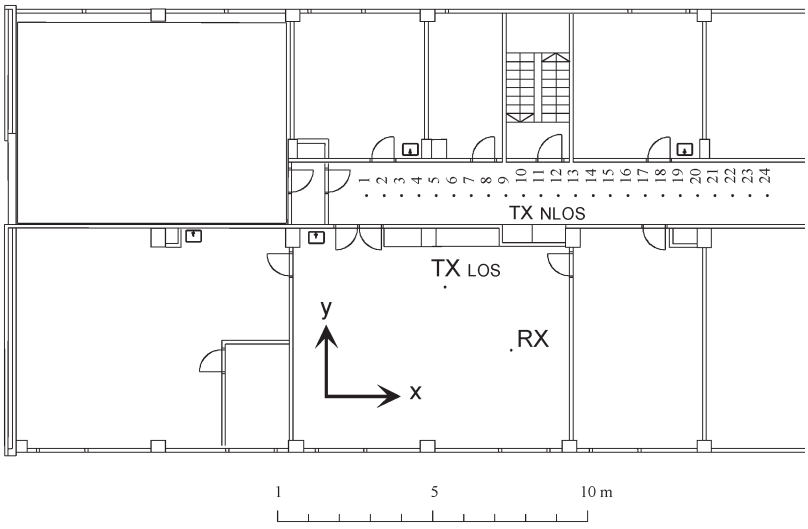

Fig. 6. Measurement location.

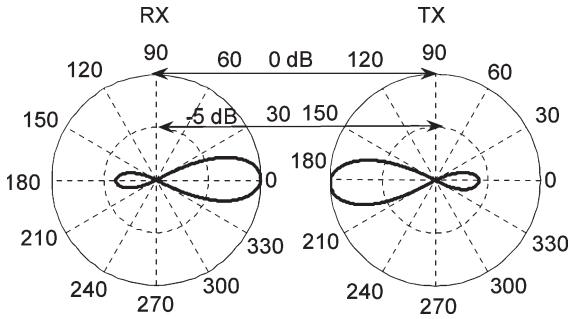

Fig. 7. TX and RX beam forming responses in LOS configuration calculated from 16 · 16 matrix. Logarithmic scale.

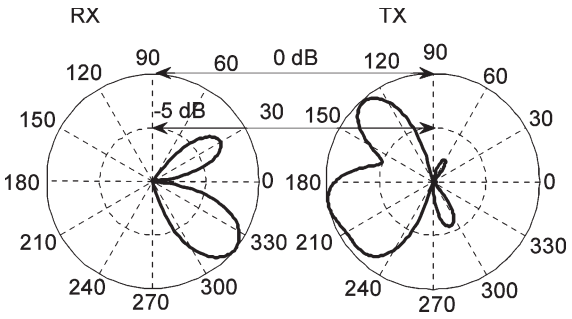

Fig. 8. TX and RX beam forming responses in LOS configuration with obstruction calculated from 16 · 16 matrix. Logarithmic scale.

each end of the radio channel. The back lobe is due to the array geometry: A sparse array has inherently high side lobes, causing ambiguity in spatial response. It is seen that the side lobe level is not significantly increased due to the nonidealities of the system. The measurement was done in 68 s.

The beam pointing rms errors calculated from successive measurements in an anechoic chamber are 0.73° in RX and 0.78° in TX. The main reason for these errors is the mechanical vibrations: The up/down converters are rather high (42 cm between the antennas and the stages) and relatively heavy (4.5 kg), and there are strong accelerations. Therefore, despite the significant attention paid to this problem, there are still residual mechanical vibrations.

Fig. 8 shows the TX and RX beam forming responses of 16 · 16 channel matrix in an obstructed LOS case with the square absorber (50 ∗ 50 cm) placed at a distance equal to the TX and RX. The antenna array configuration is shown in Fig. 4(a). As for the LOS case, the side lobes are due to the geometry of the antenna arrays. Even though the beams are quite wide due to the algorithm, it is seen that, unlike the LOS case (Fig. 7), the beams at TX and RX are pointing in directions other than the direct path between the transmitter and the receiver. Therefore, there is no direct signal from TX to RX (only reflections and diffractions on the scattering environment surrounding the measurement system).

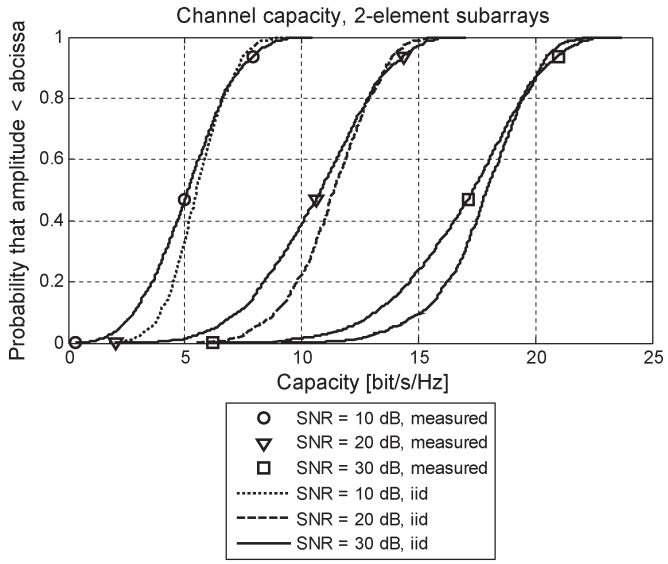

Fig. 9. Capacity of the channel in NLOS configuration and the IID MIMO Rayleigh channel, selecting two elements at TX and two elements at RX.

B. Capacity Calculation

1) Increase of the Capacity as a Function of the Number of Elements per Antenna Array: Now, it is well known that the

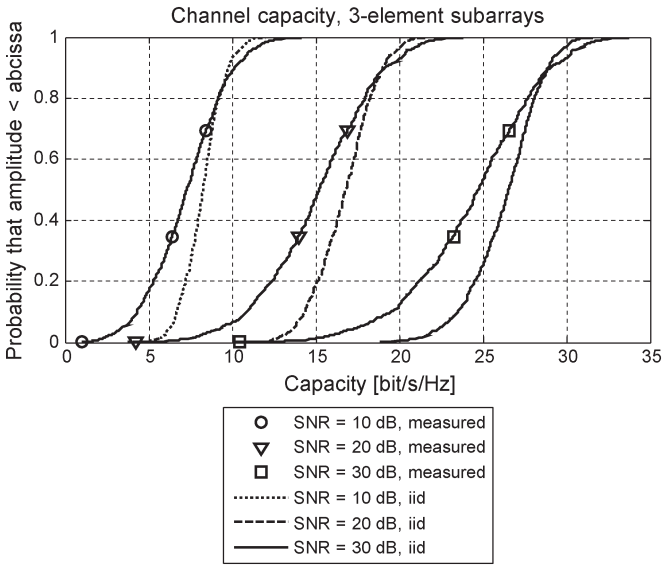

Fig. 10. Capacity of the channel in NLOS configuration and the IID MIMO Rayleigh channel, selecting three elements at TX and three elements at RX.

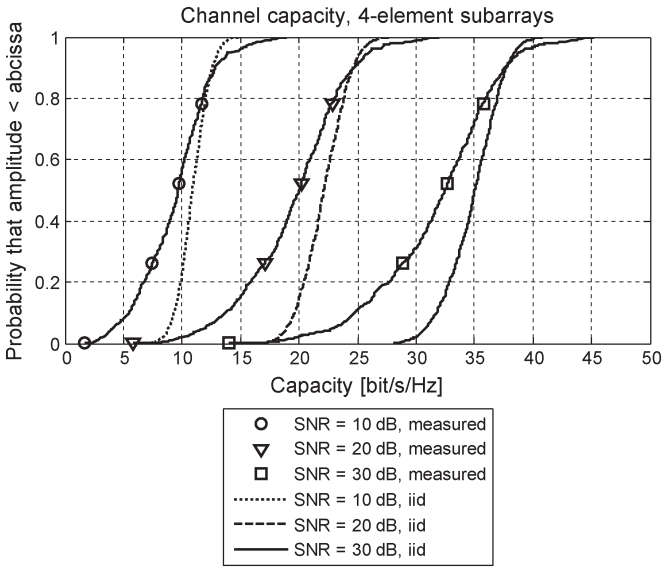

Fig. 11. Capacity of the channel in NLOS configuration and the IID MIMO Rayleigh channel, selecting four elements at TX and four elements at RX.

capacity of a MIMO system with N uncorrelated sources with equal power is given by

$$C = \log_2 \left[\det \left(I_M + \frac{\rho}{N} \mathrm{H}\mathrm{H}^* \right) \right] \text{ bit/s/Hz} \qquad (1)$$

where H is the $M \times N$ channel matrix, $(^*)$ means transpose conjugate, and ρ is the signal-to-noise ratio (SNR) at any RX antenna [10]. Foschini and Gans [10] demonstrated that the capacity in (1) increases linearly with $m = \min(M, N)$ when the sources are uncorrelated. The capacity is calculated for various antenna array sizes $[2 \cdot 2]$, $[3 \cdot 3]$, $[4 \cdot 4]$, and $[5 \cdot 5]$ in order to compare the experimental results to the theory and to see how close these results can be to the theoretical limit. The capacities of the MIMO channels are calculated as in [11]. The space between two elements is λ ($\lambda = 4.89$ mm at 61.3 GHz).

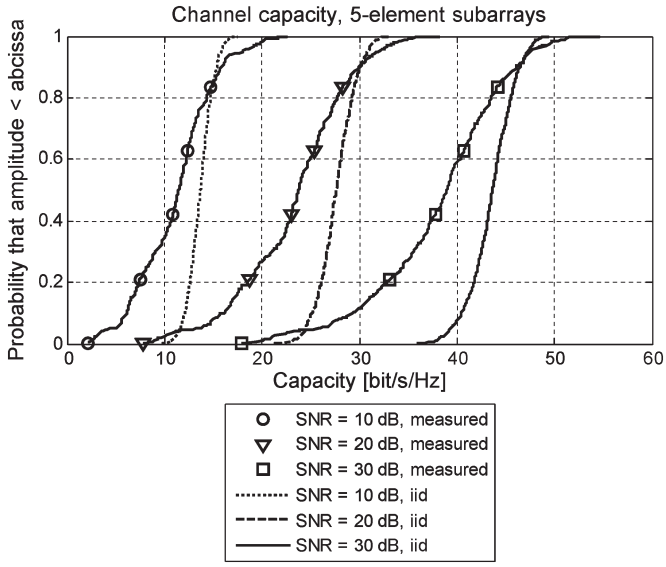

Fig. 12. Capacity of the channel in NLOS configuration and the IID MIMO Rayleigh channel, selecting for each capacity, five elements at TX and five elements at RX.

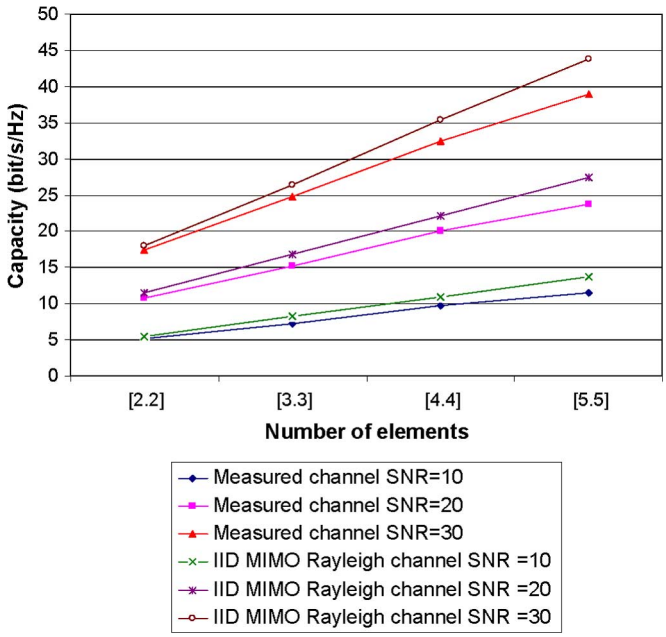

Fig. 13. Median capacity of the channel in NLOS configuration and the IID MIMO Rayleigh channel, selecting two, three, four, and five elements at TX and RX.

The capacities are calculated from the NLOS measurements where the receiver was kept in a room, and the transmitter was moved to 24 different positions in a corridor (Fig. 6). The 25-element antenna arrays depicted in Fig. 4(b) were used.

To calculate the MIMO capacity, as shown in Fig. 9, for various SNR, pairs of elements at the transmitter and pairs of elements at the receiver are selected in order to obtain 1920 different channel matrices of the size $[2 \cdot 2]$. For comparison, the capacity of the IID MIMO Rayleigh channel defined in [12] is plotted in the same figure.

The MIMO capacities for $[3 \cdot 3]$, $[4 \cdot 4]$, and $[5 \cdot 5]$ element channel matrices are shown in Figs. 10–12, respectively,

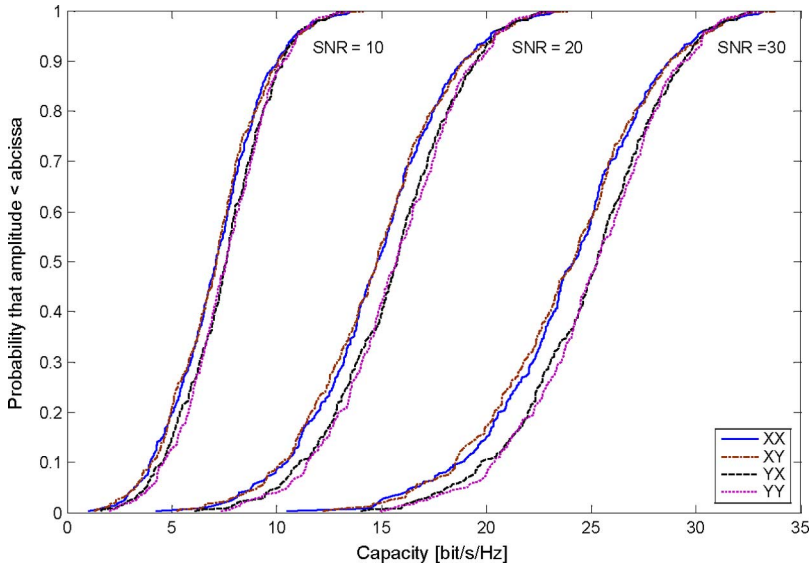

Fig. 14. Comparison of the capacity as a function of the orientation of the elements, in NLOS configuration, using three elements at both TX and RX.

together with the capacity of the IID MIMO Rayleigh channels for the same number of elements. The capacity calculated for three elements at both TX and RX is done using 1440 different channel matrices of size [3 · 3]. The capacity calculated for four elements at both TX and RX is done using 960 different channel matrices of the size [4 · 4], and to calculate the capacity for five elements at both TX and RX, 480 different channel matrices of the size [5 · 5] are used. It can be seen that the median value of the capacity of the measured channel is always smaller than the one of the capacity of the IID MIMO Rayleigh channel. Furthermore, it has to be noticed that this difference is increasing as the SNR increases and as the number of chosen element increases.

Fig. 13 shows the median value of the capacity of the measured channel as well as that of the IID MIMO Rayleigh channel, depending on the number of elements per array—[2 · 2], [3 · 3], [4 · 4], and [5 · 5]—with three different SNR values: 10, 20, and 30 dB. One can see that the capacity of the measured channel is slightly lower than the one of the IID MIMO Rayleigh channel. The difference between the experimental results and the theoretical values increases as the SNR increases. This difference is mainly due to the facts that the distance between the elements is not infinite but is equal to one wavelength, that the angles of arrival and departure of the signals are not uniformly distributed, and that the channel is not ideal (finite number of multipaths).

2) Effect of the Antenna Array Orientation on the Capacity: To determine the effect of the orientation of the antenna arrays on the capacity, the elements are selected along the x-axis or the y-axis as follows: xx, xy, yx, and yy.

The first letter refers to the transmitter orientation and, the second one to the receiver orientation, as shown in Fig. 6. For example, xy means that the elements are selected at the transmitter along the x-axis and at the receiver along the y-axis. In Fig. 14, it can be seen that the capacity can vary up to 1.2 bit/s/Hz, depending on the orientation of the elements. It is shown that the main differences appear when the orientation of the elements is changed at the transmitter, which is in the corridor. There is almost no variation when we change the orientation of the elements at the receiver, which is in the room. The highest capacities are found when the elements at the transmitters are selected along the y-axis (perpendicular to the corridor), regardless of the orientation of the elements at the receiver. This comes from the fact that the room where the receiver is placed contains many devices (computers, VNA, signal generators, etc.) and is rich in scattering elements. Therefore, the angular distribution at the receiver is much more uniform than the one at the transmitter, which is placed in the corridor. Consequently, the effects of the receiver orientation on the capacity are quite limited.

VI. Conclusion

A millimeter-wave MIMO channel measurement system developed in the Radio Laboratory of Helsinki University of Technology was presented in this paper. This MIMO measurement system works at 61.3 GHz and is based on a channel sounder and virtual antenna arrays. Measurements in the LOS and the LOS obstructed with a 16-element array at both the transmitter and at the receiver are reported, as well as measurements in NLOS using a 25-element array at both the transmitter and receiver. From the LOS measurements, DoA and DoD are estimated. From the NLOS measurements, the MIMO channel capacity is calculated for various numbers of elements per array: [2 · 2], [3 · 3], [4 · 4], and [5 · 5]. It is seen that the capacity increases almost linearly as a function of the number of elements, as stated in theory [10]. Finally, the effects of the orientation of the elements on the capacity are reported.

Acknowledgment

The authors would like to thank J. Koivunen and P. Suvikunnas for their help in this work.

REFERENCES

[1] P. F. M. Smulders, "Exploiting the 60 GHz band for local wireless multimedia access: Prospect and future directions," *IEEE Commun. Mag.*, vol. 40, no. 1, pp. 140–147, Jan. 2002.

[2] P. F. M. Smulders and A. G. Wagemans, "Frequency-domain measurement of the millimeter wave indoor radio channel," *IEEE Trans. Instrum. Meas.*, vol. 44, no. 6, pp. 1017–1022, Dec. 1995.

[3] S. J. Howard and K. Pahlavan, "Measurement and analysis of the indoor radio channel in the frequency domain," *IEEE Trans. Instrum. Meas.*, vol. 39, no. 5, pp. 751–755, Oct. 1990.

[4] J. Kivinen, P. Suvikunnas, D. Perez, C. Herrero, K. Kalliola, and P. Vainikainen, "Characterization system for MIMO channels," in *Proc. 4th Int. Symp. WPMC*, Aalborg, Denmark, Sep. 9–12, 2001, pp. 159–162.

[5] H. Oezcelik, M. Herdin, and H. Hofstetter, "Indoor 5.2 GHz MIMO measurement campaign," *COST Temporary Document TD (04) 174*, Sep. 20–22, 2004, Duisburg, Germany.

[6] J. Kivinen, T. O. Korhonen, P. Aikio, R. Gruber, P. Vainikainen, and S.-G. Haggman, "Wideband radio channel measurement system at 2 GHz," *IEEE Trans. Instrum. Meas.*, vol. 48, no. 1, pp. 39–44, Feb. 1999.

[7] J. Kivinen, P. Kangaslahti, M. Kärkkäinen, and X. Zhao, "Wideband radio channel sounder extension to 60 GHz frequency range," in *Proc. 31st Eur. Microw. Conf.*, London, U.K., Sep. 25–27, 2001, pp. 305–308.

[8] J. Laurila, K. Kalliola, M. Toeltsch, K. Hugl, P. Vainikainen, and E. Bonek, "Wideband 3D characterization of mobile radio channels in urban environment," *IEEE Trans. Antennas Propag.*, vol. 50, no. 2, pp. 233–243, Feb. 2002.

[9] D. S. Baum and H. Bölcskei, "Impact of phase noise on MIMO channel measurement accuracy," in *Proc. IEEE VTC4—Fall*, Los Angeles, CA, Sep. 26–29, 2004, pp. 1614–1618.

[10] J. G. Foschini and M. J. Gans, "On limits of wireless communications in a fading environment when using multiple antennas," *Wirel. Pers. Commun.*, vol. 6, no. 3, pp. 311–335, Mar. 1998.

[11] K. Sulonen, P. Suvikunnas, L. Vuokko, J. Kivinen, and P. Vainikainen, "Comparison of MIMO antenna configurations in picocell and microcell environments," *IEEE J. Sel. Areas Commun.—Special Issue MIMO Systems and Application*, vol. 21, no. 5, pp. 703–712, Jun. 2003.

[12] J. G. Foschini, "Layered space-time architecture for wireless communication in a fading environment when using multi-element antennas," *Bell Labs Tech. J.*, vol. 1, no. 2, pp. 41–59, 1996.

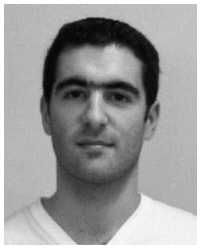

Sylvain Ranvier was born in Melun, France, in 1980. He received the "diplôme d'ingénieur EFREI" (M.Sc.) degree in electronics and telecommunication from Ecole Française d'Electronique et d'Informatique (EFREI), Villejuif, France, in 2003 and the Licentiate of Science (Technology) degree in electrical engineering from Helsinki University of Technology (TKK), Espoo, Finland, in 2005.

Since 2003, he has been working in the Radio Laboratory, TKK, as a Researcher. During 2005 to 2006, he was visiting the University of Nice-Sophia Antipolis, Nice, France. His current research interests include radio channel measurements and millimeter-wave antenna design.

Jarmo Kivinen was born in Helsinki, Finland, in 1965. He received the Master of Science in Technology, Licentiate of Science in Technology, and Doctor of Science in Technology degrees from Helsinki University of Technology (HUT), Espoo, Finland, in 1994, 1997, and 2001, respectively, all in electrical engineering.

He worked as a Research Engineer and Project Leader with the Radio Laboratory of HUT from 1994 to 2005 and as an RF Design Engineer with Nokia Telecommunications from 1995 to 1996. Since 2006, he has been working as a Specialist at Elektrobit OY, Kauniainen, Finland. His main fields of interest are in multidimensional radio propagation channel measurement and modeling techniques, and RF techniques in radio communications.

Pertti Vainikainen (S'87–M'91) received the Master of Science in Technology, Licentiate of Science in Technology, and Doctor of Science in Technology degrees from Helsinki University of Technology (TKK), Espoo, Finland, in 1982, 1989, and 1991, respectively.

From 1992 to 1993, he was an Acting Professor of radio engineering; since 1993, he has been an Associate Professor of radio engineering; and since 1998, he has been a Professor in radio engineering, all in the Radio Laboratory of TKK. From 1993 to 1997, he was the Director of the Institute of Radio Communications (IRC) of TKK, and in 2000, he was a Visiting Professor with Aalborg University, Aalborg, Denmark. His main fields of interest include antennas and propagation in radio communications and industrial measurement applications of radio waves. He has authored or coauthored of six books and about 240 refereed international journals or conference publications and is the holder of seven patents.